Kinetics and mechanism of the bleaching of a triarylmethane dye by hydrogen peroxide and water: evidence for intramolecular base catalysis

D. Martin Davies* and Alexei U. Moozyckine

Division of Chemical Sciences, School of Applied and Molecular Sciences, University of Northumbria at Newcastle, Newcastle upon Tyne, UK NE1 8ST

Received (in Cambridge, UK) 10th February 2000, Accepted 18th April 2000
Published on the Web 23rd May 2000

This work describes the ionisation of the triarylmethane dye Green S and the kinetics of its oxidation by hydrogen peroxide over a wide range of pH. Spectrophotometric titration yields pK_a values for the equilibria $\mathbf{D}^{2-} + H_2O = \mathbf{D}(OH)^{3-} + H^+$, $H\mathbf{D}^- = \mathbf{D}^{2-} + H^+$, and $H_2\mathbf{D} = H\mathbf{D}^- + H^+$ of 11.72, 7.66, and 1.31 respectively. The forward rate constant for the first reaction is 1.3×10^{-4} s^{-1}. The UV-visible spectrum of $H\mathbf{D}^-$ indicates that the *ortho*-O^- substituent is protonated. The rate constant for the reaction of $\mathbf{D}^{2-}$ and HOO^-, determined at high pH, is 0.31 dm^3 mol^{-1} s^{-1}. Rate constants for the reactions of $\mathbf{D}^{2-}$ and HOO^- associated with one, two and three protons, respectively, have been estimated from the pH dependence of the reaction. From the application of the transition-state pK_a approach and consideration of the changes in the UV-visible spectra during the reactions, the rate constants have been assigned to the reactions of H_2O_2 and $\mathbf{D}^{2-}$ (0.48 dm^3 mol^{-1} s^{-1}); H_2O_2 and $H\mathbf{D}^-$ or $H_3O_2^+$ and $\mathbf{D}^{2-}$ (respective upper limits, 5.7×10^{-6} or 1.3×10^7 dm^3 mol^{-1} s^{-1}) and $H_3O_2^+$ and $H\mathbf{D}^-$ (5.1×10^2 dm^3 mol^{-1} s^{-1}). Comparisons between these rate constants and published rate constants for alkali and peroxide bleaching of similar triarylmethane dyes show the exceptionally high reactivity of $\mathbf{D}^{2-}$ toward H_2O and H_2O_2. This is attributed to intramolecular base catalysis by the *ortho*-O^- substituent of $\mathbf{D}^{2-}$ and is discussed in terms of the position of the catalytic site and the pK_a of its conjugate acid. The relevance of this work to oxygen atom transfer catalysts is considered.

Introduction

Chemical oxidation methods in solution hold promise for the treatment of industrial wastewater or polluted waters containing non-biodegradable materials. Dyes are appropriate substrates for chemical oxidation studies because many are not amenable to conventional activated sludge treatment and because of the large quantities contained in textile effluents.[1] Triarylmethane dyes are of particular interest since they enter the aquatic environment and have been well-studied by physical organic chemists.[2,3] Rate and equilibrium constants for the reactions of polyarylmethane dyes and a wide range of nucleophiles (including the hydroperoxide anion) are usually remarkably well correlated.[4] Hydrogen peroxide is the chemical oxidant of choice from an environmental viewpoint.

Unfortunately, in the absence of added catalysts hydrogen peroxide is effective only at extremes of pH that are unsuitable for environmental water treatment. There are two main types of redox catalysts for hydrogen peroxide. Fenton-type catalysts donate a single electron to the peroxide and need a reduction step, in practice usually photochemical or electrochemical, to complete the catalytic cycle.[5] Oxygen atom transfer catalysts, however, do not require exogenous electron donors. This type includes the peroxidase enzymes that depend upon concerted general base catalysis to remove a proton from hydrogen peroxide during the formation of the active intermediate at neutral pH.[6] In these proteins the general base catalyst is the imidazole group (pK_a of the conjugate imidazolinium ion, 7.0) of the histidine distal to the peroxide-binding site. Simple chemical oxygen transfer catalysts that depend only upon the pre-equilibrium ionisation of hydrogen peroxide require a high reaction pH, approaching the pK_a of hydrogen peroxide, in order to form an active intermediate analogous to the enzyme system.[7] This is problematic if strongly alkali reaction conditions are to be avoided.

The above problem with simple catalytic systems is also encountered for uncatalysed reactions of electrophilic substrates and hydrogen peroxide, where the hydroperoxide anion, HOO^-, is normally the reactive species and high pH is required. This is so for several dyes including the hydrazone tautomers of hydroxyazo dyes,[8] Alizarin, Crocetin, and the triphenylmethane dye, phenolphthalein.[9,10] The subject of the present paper is also a triarylmethane dye, Green S. This dye does not require a high pH to react with hydrogen peroxide. This is attributed to intramolecular base catalysis occurring at the *ortho*-O^- neighbouring the central carbon reaction site. The pK_a of the conjugate acid of the catalytic O^- is 7.66. This is similar to the pK_a of the conjugate acid of the catalytic imidazole in peroxidase, which is significant for catalysis involving hydrogen peroxide.[6] The *ortho*-O^- of Green S also confers the dye with the peculiar property that during alkali bleaching the rate constant for the approach to equilibrium increases with increasing hydrogen ion concentration. The pH dependence of the kinetics of dye oxidation by hydrogen peroxide is interpreted mechanistically using the transition state pK_a approach of Kurz.[11]

Green S (Lissamine Green B, Acid Green 50, Wool Green S, C.I. 44090) belongs to the Victoria Blue series, which has one 1-naphthyl and two phenyl residues attached to the central carbon in a non-coplanar manner, resembling a three-bladed propeller. It has been used for a long time as a food colourant, and recently as a low toxicity stain towards membrane-damaged epithelial cells.[12] It is also used as a selective spectrophotometric reagent for the determination of residual chlorine dioxide in water treatment.[13]

DOI: 10.1039/b001156h

Experimental

Green S was obtained from Sigma (Lissamine Green B) and was of the best commercially available quality and used without further purification. Hydrogen peroxide, 30 wt%, puriss., non-stabilised, was obtained from Fluka and 27.5 wt%, stabilised, from Aldrich. The disodium salt of EDTA was obtained from BDH and ethylenediaminetetramethylenephosphonic acid (EDTMP·H_2O, 92:8) from Warwick International Ltd. All other reagents used for preparing buffers were of analytical grade (Aldrich, Merck). Solutions were made up in distilled water unless stated otherwise.

Measurements were carried out at 25 ± 0.2 °C in buffered aqueous solutions of ionic strength 0.10 mol dm^{-3} over the following pH ranges: KCl + HCl or KCl + HNO_3, 1.0–4.3; CH_3COONa + CH_3COOH, 3.8–5.5; Na_2HPO_4 + NaH_2PO_4, 6.3–8.7; Na_2CO_3 + $NaHCO_3$, 9.2–10.7; Na_2HPO_4 + NaOH, 11.2–11.8; KCl + NaOH, 10.7–12.9. A Metrohm 702 SM Titrino calibrated with Hydrion™ buffers pH 4.00, 7.00 and 10.00 was used to measure pH. The concentration of Green S was usually 1.25×10^{-5} mol dm^{-3}, but some experimental series involved dye concentrations of 1.25×10^{-6} and 8.75×10^{-5} mol dm^{-3}. The UV/vis spectra of the dye at various pH values were obtained using a Pharmacia Biotech Ultraspec 2000 spectrophotometer with a thermostatic cell-holder. Above pH 9 spectra were obtained immediately after mixing solutions of the dye and buffer and then at appropriate intervals until the completion of the equilibration of the alkali bleaching process. Spectral changes during peroxide bleaching of the dye were followed using the Pharmacia spectrophotometer or an Applied Photophysics SX-17MV stopped-flow instrument. Generally, at least six different concentrations of hydrogen peroxide, ranging from 0.005 mol dm^{-3} to 0.20 mol dm^{-3}, were used. Hydrogen peroxide solutions were made up in distilled water to avoid any decomposition prior to initiation of the reaction, especially at high pH. Green S solutions were made up in double strength buffer, immediately before use if above pH 9, unless stated otherwise. Equal volumes of the solutions were mixed to initiate the reaction. For alkali bleaching pseudo-first-order rate constants, k_ψ, were determined from the slopes of plots of ln $(A - A_\infty)$ against time using linear regression, where A is the absorbance at the wavelength of maximum absorbance of the dye, 615 nm. For peroxide bleaching reactions the pseudo-first-order rate constants were obtained similarly, using wavelengths between 615 nm and 635 nm depending upon the pH. For the very slow reactions, less than thirty percent of the reaction was followed and A_∞ was assumed to be zero. For the relatively rapid reaction at pH 1.2 the first-order rate constants were calculated from initial rates for the reason described in the Results section. Reaction solutions below pH 5 contained 4×10^{-5} mol dm^{-3} EDTA as a precautionary measure to eliminate trace metal catalysed bleaching that would be significant at very low rates. At higher pH the pseudo-first-order rate constants were generally obtained by non-linear regression of the mono-exponential decrease in absorbance with time. The second order rate constant under the experimental conditions, k_{obs}, was calculated as the slope ± standard deviation of a linear regression of the pseudo-first order rate constant *versus* hydrogen peroxide concentration.

Results

Acid dissociation constants of Green S

Fig. 1 shows the spectra of Green S after equilibration at various pH values. Differences in the UV region below 250 nm are due to the different buffers used. Fig. 1a shows the drop in absorbance of a bright blue species, $\mathbf{D}^{2-}$ at increasing pH values above 10. This corresponds to alkali bleaching and the formation of the colourless carbinol form of the dye, $\mathbf{D}(OH)^{3-}$. Fig. 1b shows the changes between pH values of 5 and 9, where the absorbance of the major band decreases slightly and the wavelength maximum shifts about 20 nm to a shorter wavelength, 615 nm, with the appearance of a peak at 399 nm. This corresponds to a colour change from the greenish-teal species, $H\mathbf{D}^-$, to the bright blue species, $\mathbf{D}^{2-}$. Fig. 1c shows the drop in absorbance of the major band of the greenish-teal species and an increase in the broad band around 400 nm to give a light yellow species, $H_2\mathbf{D}$, at decreasing pH values below 2. The structural assignments of the species, shown in Scheme 1, are described in the Discussion section.

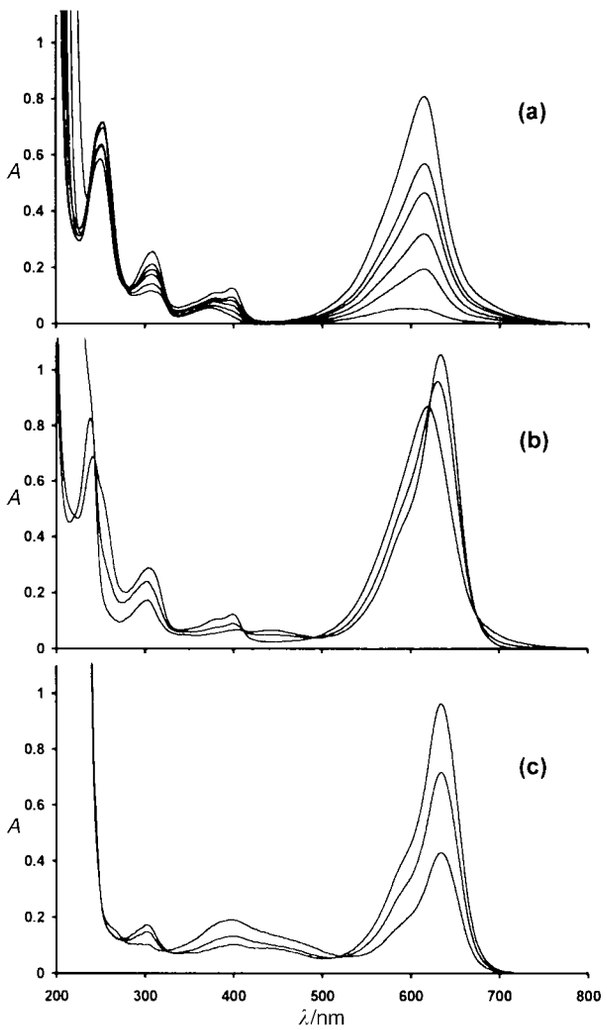

Fig. 1 Absorption spectra of 12.5×10^{-6} mol dm^{-3} Green S at 25 °C in buffers of ionic strength 0.10 mol dm^{-3} at the following pH values, in order of decreasing absorbance of the band *ca.* 600 nm: (a) 10.40, 11.39, 11.61, 11.87, 12.20, 12.79; (b) 5.31, 7.26, 8.16; (c) 2.00, 1.56, 1.17.

Fig. 2 shows the pH dependence of the absorbance of Green S at four different wavelengths. Above pH 9 the filled points represent measurements made immediately after mixing solutions of the dye and buffer whereas the open points represent measurements made after alkali bleaching had reached equilibrium. The data shown in Fig. 2, together with corresponding data at the additional wavelengths 300 nm, 444 nm, 580 nm, 616 nm, and 653 nm (omitted from Fig. 2 for clarity) were used to determine the first three of the acid dissociation constants defined by the equilibria shown in eqns. (1) to (4). The absorbance A^{λ_i} at wavelength, λ_i, is given by eqn. (5) where $\varepsilon_X^{\lambda_i}$ is the

$$\mathbf{D}^{2-} + H_2O \overset{K_{H_2O}}{\rightleftharpoons} \mathbf{D}(OH)^{3-} + H^+ \quad (1)$$

$$H\mathbf{D}^- \overset{K_{D1}}{\rightleftharpoons} \mathbf{D}^{2-} + H^+ \quad (2)$$

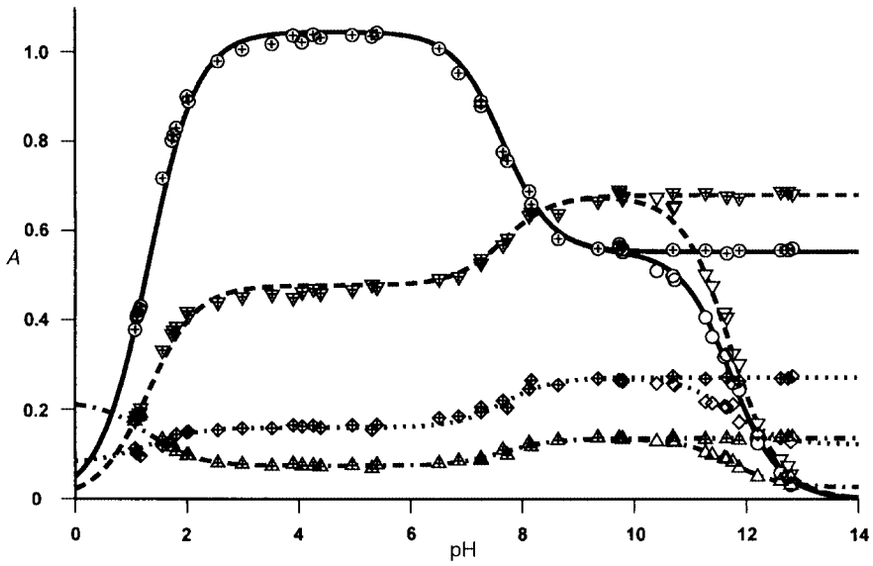

Fig. 2 Dependence upon pH of the absorbance of Green S, conditions as for Fig. 1; circles, 635 nm; triangles pointed down, 598 nm; diamonds, 308 nm; triangles pointed up, 399 nm. The open symbols correspond to the points where Green S has been alkali bleached (infinity values). The curves represent best data fits to eqns. (7) and (8).

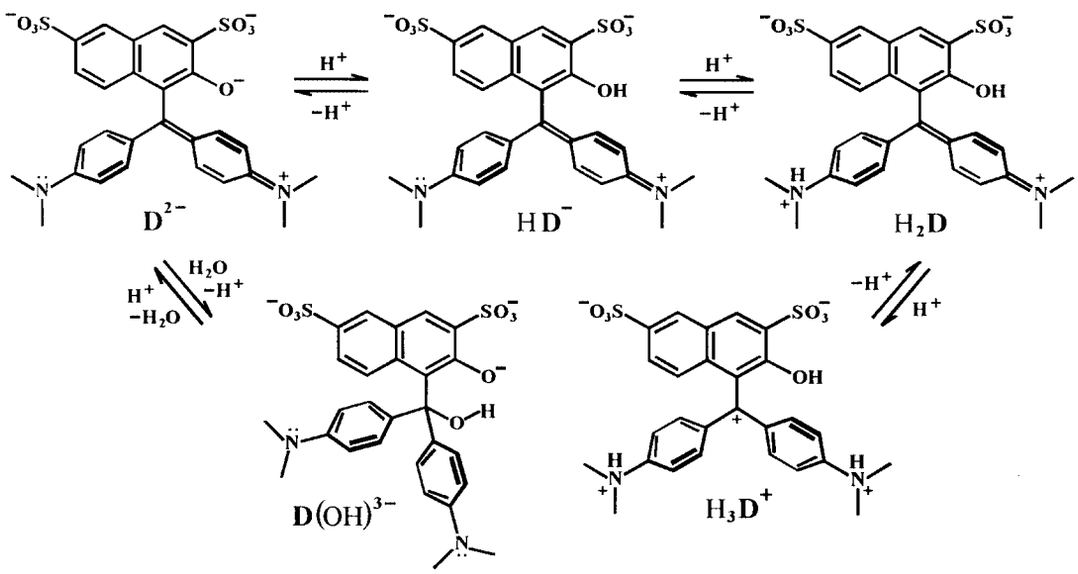

Scheme 1

$$H_2\mathbf{D} \overset{K_{D2}}{\rightleftharpoons} H\mathbf{D}^- + H^+ \quad (3)$$

$$H_3\mathbf{D}^+ \overset{K_{D3}}{\rightleftharpoons} H_2\mathbf{D} + H^+ \quad (4)$$

$$A^{\lambda_i} = \varepsilon^{\lambda_i}_{H_3D^+}[H_3\mathbf{D}^+] + \varepsilon^{\lambda_i}_{H_2D}[H_2\mathbf{D}] + \varepsilon^{\lambda_i}_{HD^-}[H\mathbf{D}^-] + \varepsilon^{\lambda_i}_{D^{2-}}[\mathbf{D}^{2-}] + \varepsilon^{\lambda_i}_{D(OH)^{3-}}[\mathbf{D}(OH)^{3-}] \quad (5)$$

extinction coefficient of the dye species X. The expressions for the equilibrium constants corresponding to the equilibria shown in eqns. (1) to (4), together with the mass conservation eqn. (6) are substituted into eqn. (5) to give an expression for the dependence of the absorbance on $[H^+]$ as follows. Since there is no evidence for the species $H_3\mathbf{D}^+$ over the pH range shown in Fig. 2 and $\mathbf{D}(OH)^{3-}$ is negligible immediately after mixing solutions of the dye and buffer then the concentrations of these species were set to zero in eqn. (6) and eqn. (7) obtained.

$$[\text{Dye}]_T = [H_3\mathbf{D}^+] + [H_2\mathbf{D}] + [H\mathbf{D}^-] + [\mathbf{D}^{2-}] + [\mathbf{D}(OH)^{3-}] \quad (6)$$

$$\frac{A^{\lambda_i}}{[\text{Dye}]_T} = \frac{\varepsilon^{\lambda_i}_{H_2D}[H^+]^2 + K_{D2}\varepsilon^{\lambda_i}_{HD^-}[H^+] + K_{D1}K_{D2}\varepsilon^{\lambda_i}_{D^{2-}}}{[H^+]^2 + K_{D2}[H^+] + K_{D1}K_{D2}} \quad (7)$$

Alternatively, for measurements made after alkali bleaching had reached equilibrium only the concentration of $H_3\mathbf{D}^+$ was set to zero and eqn. (8) obtained. Fitting eqn. (7) to the appropriate data yielded values of K_{D1} and K_{D2}. These were substituted into eqn. (8), which was used to obtain K_{H_2O} using

$$\frac{A^{\lambda_i}}{[\text{Dye}]_T} = \frac{\varepsilon^{\lambda_i}_{H_2D}[H^+]^3 + K_2\varepsilon^{\lambda_i}_{HD^-}[H^+]^2 + K_{D1}K_{D2}\varepsilon^{\lambda_i}_{D^{2-}}[H^+] + K_{H_2O}K_{D1}K_{D2}\varepsilon^{\lambda_i}_{D(OH)^{3-}}}{[H^+]^3 + K_{D2}[H^+]^2 + K_{D1}K_{D2}[H^+] + K_{H_2O}K_{D1}K_{D2}} \quad (8)$$

the alkali bleached equilibrium data. The corresponding values of pK_{H_2O}, pK_{D1} and pK_{D2} are 11.72, 7.66 and 1.31.

Since there is no evidence for the species $H_3\mathbf{D}^+$ under the conditions of the kinetic experiments, nor, indeed was there any evidence in 10 mol dm^{-3} HCl or HNO_3 (results not shown), then this indicates that $pK_{D3} \leq -1$.

Alkali bleaching of Green S

Fig. 3 shows the changes in the absorption spectrum of Green S

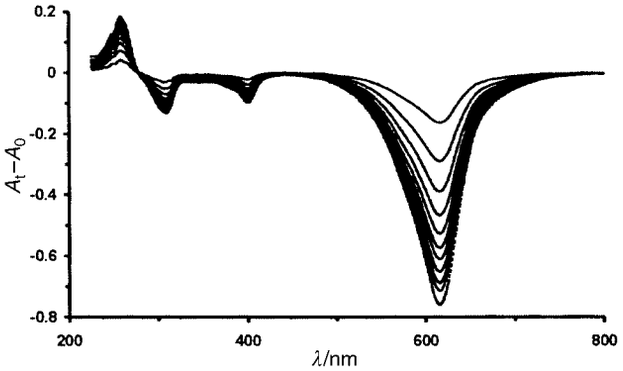

Fig. 3 The changes in the absorption spectra of 12.5×10^{-6} mol dm^{-3} Green S during alkali bleaching at pH 12.42, ionic strength 0.10 mol dm^{-3} after the following times in minutes: 32, 62, 92, 122, 152, 182, 212, 257, 317, 392, 2970 (dotted line).

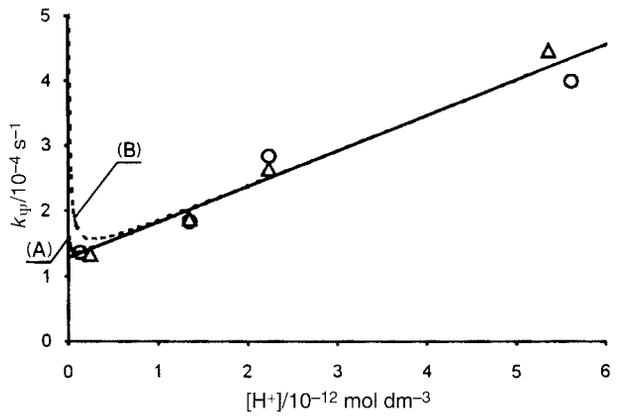

Fig. 4 Dependence upon hydrogen ion concentration of the observed first-order rate constant for the alkali bleaching of Green S at ionic strength 0.10 mol dm^{-3}. The circles correspond to [Green S] = 12.5×10^{-6} mol dm^{-3}, the triangles to [Green S] = 2.5×10^{-6} mol dm^{-3}. The curves (A), (B) represent simulations using eqn. (11) with k_{HO^-} set to 4×10^{-5} and 4×10^{-4} dm^3 mol^{-1} s^{-1}, respectively. The straight line represents the best data fit to eqn. (11) with k_{HO^-} set to zero.

during alkali bleaching at pH 12.42. The intensity of the three longer wavelength bands drops and only the band centred at 259 nm increases in absorbance, with an isosbestic point at 278 nm. Plots of ln $(A - A_\infty)$ against time are linear for at least four half-lives at all pHs studied. The observed pseudo-first-order rate constants, k_ψ, for the attainment of equilibrium, obtained from the slopes of the plots are independent of the concentration of the dye and are plotted against the hydrogen ion concentration in Fig. 4. The reversible reactions of $\mathbf{D}^{2-}$ with water and hydroxide ion, respectively are shown in eqns. (9) and (10) and the corresponding expression for k_ψ is given by eqn. (11).

$$\mathbf{D}^{2-} + H_2O \underset{k_{-H_2O}}{\overset{k_{H_2O}}{\rightleftharpoons}} \mathbf{D}(OH)^{3-} + H^+ \quad (9)$$

$$\mathbf{D}^{2-} + HO^- \underset{k_{-HO^-}}{\overset{k_{HO^-}}{\rightleftharpoons}} \mathbf{D}(OH)^{3-} \quad (10)$$

$$k_\psi = k_{H_2O} + k_{-HO^-} + k_{-H_2O}[H^+] + k_{HO^-}[HO^-] \quad (11)$$

Inspection of Fig. 4 shows that the k_{HO^-} term in eqn. (11) is insignificant, and linear regression yields a value of k_{-H_2O} of $(5.46 \pm 0.45) \times 10^7$ dm^3 mol^{-1} s^{-1} and an intercept of $(1.27 \pm 0.14) \times 10^{-4}$ s^{-1}. Fig. 4 also shows simulations where, in addition to the previous values, k_{HO^-} is set to 4×10^{-5} and 4×10^{-4} dm^3 mol^{-1} s^{-1}, respectively, for curves A and B. The value of k_{HO^-} used for curve B represents a reasonable upper limit. Now consideration of the thermodynamic cycle in Scheme 2 yields

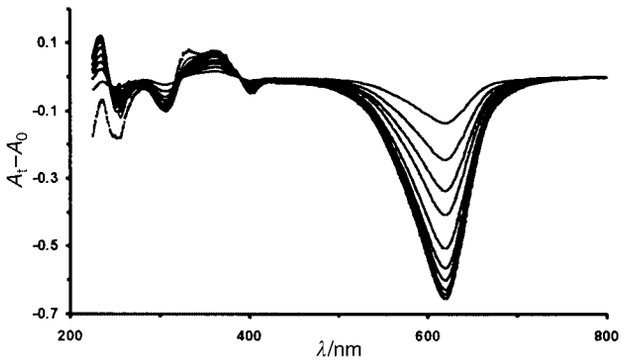

Fig. 5 The changes in the absorption spectra of 12.5×10^{-6} mol dm^{-3} Green S during bleaching with 0.020 mol dm^{-3} hydrogen peroxide at pH 8.08, ionic strength 0.10 mol dm^{-3} after the following times in seconds: 30, 54, 78, 102, 150, 198, 246, 318, 390, 942, 12600 (dotted line).

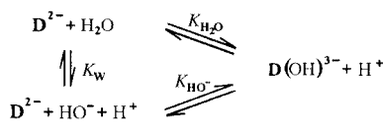

Scheme 2

the relationship in eqn. (12), where K_w is the ion product of

$$K_{H_2O} = K_W K_{HO^-} \quad (12)$$

water, 1×10^{-14} dm^6 mol^{-2} at 25 °C, and application of the principle of microscopic reversibility converts eqn. (12) to eqn. (13). Using the chosen upper limit for k_{HO^-}, an upper limit

$$\frac{k_{H_2O}}{k_{-H_2O}} = K_W \frac{k_{HO^-}}{k_{-HO^-}} \quad (13)$$

of 1.7×10^{-7} s^{-1} is calculated for k_{-HO^-}. This is negligible compared with the value of the intercept $(1.27 \pm 0.14) \times 10^{-4}$ s^{-1} in Fig. 4, which therefore represents the value of k_{H_2O}. The quotient of the values of k_{H_2O} and k_{-H_2O} is $(2.33 \pm 0.32) \times 10^{-12}$ mol dm^{-3} comparable to the value of 1.91 x10^{-12} determined from the equilibrium measurements in the previous section.

Hydrogen peroxide bleaching of Green S

Preliminary experiments at higher pHs showed that the decomposition of hydrogen peroxide was considerably slower than the oxidation of Green S under the same conditions. Moreover, there was no difference between the bleaching data obtained using distilled and triple distilled water or stabilised and non-stabilised hydrogen peroxide solutions, and the addition of the sequestering agents EDTA and EDTMP also had no effect at concentrations of 4.0×10^{-5} mol dm^{-3}. Hence, all further experiments above pH 5 were carried out without the use of any chelating or stabilising agents. At lower pH, 4.0×10^{-5} mol dm^{-3} EDTA was used as a precautionary measure although its omission at pH 1.8 did not cause an increase in the measured rate constant (results not shown).

Fig. 5 shows changes in the absorption spectrum of Green S during hydrogen peroxide bleaching at pH 8.1. The intensity of the visible-wavelength bands drops and there is an increase in absorbance at lower wavelengths, with isosbestic points at 323 nm and 390 nm. Similar spectral scans were observed at pH values of 2.4, 5.5, 9.7 and 12.4 (results not shown). At pH 1.2, however, spectral scans were very different and although the main visible band was completely bleached the absorbance increased around 385 nm with a shoulder around 480 nm and with approximate isosbestic points at 320 nm and 525 nm. With the exception of runs at pH 1.2, plots of ln $(A - A_\infty)$ against

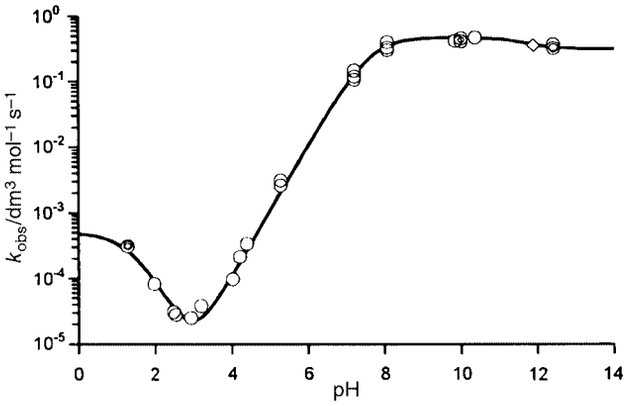

Fig. 6 Dependence upon pH of the observed second-order rate constants for the bleaching of Green S by hydrogen peroxide. Multiple points at the same pH represent different Green S concentrations. The diamond corresponds to a point where Green S has been partially alkali bleached prior to H_2O_2 bleaching at the same pH. The curve represents the best fit of eqn. (29) to the data points excluding the diamond.

time were linear for at least three half-lives or for as long as the reaction was followed and were independent of the initial concentration of the dye. At pH 1.2 the logarithmic plots did not exhibit a linear region but showed steady negative deviations from linearity with time. So the method of initial rates was used in order to get more precise first-order rate constants at this pH, in order to provide a comparison with the pseudo-first-order rate constants at other pH values. The pseudo-first-order rate constants were directly proportional to the concentration of hydrogen peroxide and second-order rate constants, k_{obs}, were obtained from the gradient. Standard deviations of k_{obs} were generally less than 5% of the best fit values. Fig. 6 shows the pH dependence of k_{obs}, on a logarithmic scale, and that the effect of concentration of $\mathbf{D}^{2-}$ is negligible. Also the presence of $\mathbf{D}(OH)^{3-}$ in mixtures containing partially alkali bleached dye has no effect on the observed rate constant for peroxide bleaching. Alkali bleaching is insignificant on the time scale of the peroxide bleaching and the results are consistent with the reaction scheme shown in eqns. (14) to (22).

$$\mathbf{D}^{2-} + HOO^- \xrightarrow{k_P^D} \text{Products} \quad (14)$$

$$H\mathbf{D}^- + HOO^- \xrightarrow{k_P^{D1}} \text{Products} \quad (15)$$

$$\mathbf{D}^{2-} + H_2O_2 \xrightarrow{k_{P1}^D} \text{Products} \quad (16)$$

$$H_2\mathbf{D} + HOO^- \xrightarrow{k_P^{D2}} \text{Products} \quad (17)$$

$$H\mathbf{D}^- + H_2O_2 \xrightarrow{k_{P1}^{D1}} \text{Products} \quad (18)$$

$$\mathbf{D}^{2-} + H_3O_2^+ \xrightarrow{k_{P2}^D} \text{Products} \quad (19)$$

$$H_3\mathbf{D}^+ + HOO^- \xrightarrow{k_P^{D3}} \text{Products} \quad (20)$$

$$H_2\mathbf{D} + H_2O_2 \xrightarrow{k_{P1}^{D2}} \text{Products} \quad (21)$$

$$H\mathbf{D}^- + H_3O_2^+ \xrightarrow{k_{P2}^{D1}} \text{Products} \quad (22)$$

Eqn. (14) represents the reaction between $\mathbf{D}^{2-}$ and HOO^-, eqns. (15) and (16) represent pathways with an additional proton in the transition state, eqns. (17)–(19) represent pathways with two additional protons in the transition state and eqns. (20)–(22), three. The scheme leads to the rate equation shown in eqn. (23).

$$-\frac{d[Dye]_T}{dt} = \left\{\begin{array}{l} k_P^D[\mathbf{D}^{2-}][HOO^-] \\ +k_P^{D1}[H\mathbf{D}^-][HOO^-] + k_{P1}^D[\mathbf{D}^{2-}][H_2O_2] \\ +k_P^{D2}[H_2\mathbf{D}][HOO^-] + k_{P1}^{D1}[H\mathbf{D}^-][H_2O_2] + k_{P2}^D[\mathbf{D}^{2-}][H_3O_2^+] \\ +k_P^{D3}[H_3\mathbf{D}^+][HOO^-] + k_{P1}^{D2}[H_2\mathbf{D}][H_2O_2] + k_{P2}^{D1}[H\mathbf{D}^-][H_3O_2^+] \end{array}\right\} \quad (23)$$

From eqn. (23) and the expressions for the acid dissociation constants of the relevant dye species, defined by the equilibria shown in eqns. (2) to (4), and the peroxide species, defined by the equilibria shown in eqns. (24) and (25), the mass conserv-

$$H_2O_2 \overset{K_{P1}}{\rightleftharpoons} HOO^- + H^+ \quad (24)$$

$$H_3O_2^+ \overset{K_{P2}}{\rightleftharpoons} H_2O_2 + H^+ \quad (25)$$

ation equation for the dye species, eqn. (6) with the concentration of $\mathbf{D}(OH)^{3-}$ set to zero, and the mass conservation equation for hydrogen peroxide, eqn. (26), the relationship

$$[H_2O_2]_T = [H_3O_2^+] + [H_2O_2] + [HOO^-] \quad (26)$$

between the observed second order rate constant, defined in eqn. (27), and $[H^+]$ that is shown in eqn. (28) is obtained. Now

$$-\frac{d[Dye]_T}{dt} = k_{obs}[Dye]_T[H_2O_2]_T \quad (27)$$

since only three points of inflection are observed in the pH dependence of k_{obs}, Fig. 6, the terms in $[H^+]^4$ and $[H^+]^5$ in the numerator of eqn. (28) (see below) are negligible over the experimental pH range. Also since only three dye species can be identified from the spectrophotometric titration, Fig. 2, this means that K_{D3}, the acid dissociation constant of $H_3\mathbf{D}^+$, is very large such that $K_{D3} \gg [H^+]$. Moreover, K_{P2} the acid dissociation constant of $H_3O_2^+$ has been estimated[14] at 5×10^4 mol dm^{-3} and so $K_{P2} \gg [H^+]$ over the experimental range. Hence the terms in $[H^+]^4$ and $[H^+]^5$ in the denominator of eqn. (28) are also negligible. The importance of the other terms in the denominator of eqn. (28) can be assessed, given the value of the pK_a of H_2O_2 (pK_{P1}, 11.6)[15] and comparing the magnitude of the various acid dissociation constants, leading to eqn. (29) where k_{0obs}, k_{1obs}, k_{2obs}, and k_{3obs} are defined in eqns. (30) to (33).

$$k_{obs} = \frac{k_{0obs} + k_{1obs}[H^+] + k_{2obs}[H^+]^2 + k_{3obs}[H^+]^3}{K_{D1}K_{D2}K_{P1} + K_{D1}K_{D2}[H^+] + K_{D2}[H^+]^2 + [H^+]^3} \quad (29)$$

$$k_{0obs} = k_P^D K_{D1}K_{D2}K_{P1} \quad (30)$$

$$k_{obs} = \frac{\left\{\begin{array}{l} k_P^D K_{D1}K_{D2}K_{P1} + (k_P^{D1}K_{D2}K_{P1} + k_{P1}^D K_{D1}K_{D2})[H^+] \\ +(k_P^{D2}K_{P1} + k_{P1}^{D1}K_{D2} + k_{P2}^D K_{D1}K_{D2}/K_{P2})[H^+]^2 \\ +(k_P^{D3}K_{P1}/K_{D3} + k_{P1}^{D2} + k_{P2}^{D1}K_{D2}/K_{P2})[H^+]^3 \\ +(k_{P1}^{D3}/K_{D3} + k_{P2}^{D2}/K_{P2})[H^+]^4 + (k_{P2}^{D3}/K_{D3}K_{P2})[H^+]^5 \end{array}\right\}}{\left\{\begin{array}{l} K_{D1}K_{D2}K_{P1} + (K_{D2}K_{P1} + K_{D1}K_{D2})[H^+] + (K_{P1} + K_{D2} + K_{D1}K_{D2}/K_{P2})[H^+]^2 \\ +(K_{P1}/K_{D3} + 1 + K_{D2}/K_{P2})[H^+]^3 + (1/K_{D3} + 1/K_{P2})[H^+]^4 + (1/K_{D3}K_{P2})[H^+]^5 \end{array}\right\}} \quad (28)$$

Table 1 Observed rate constants ($dm^3\ mol^{-1})^{n+1}\ s^{-1}$, for pathways involving n additional protons in the transition state, the corresponding upper limits for the bimolecular rate constants, $dm^3\ mol^{-1}\ s^{-1}$, and the negative logarithms of the transition state acid dissociation constants

n	$k_{n\mathrm{obs}}$	$k_{\mathrm{P}}^{\mathrm{D}n}$	$k_{\mathrm{P1}}^{\mathrm{D}n-1}$	$k_{\mathrm{P2}}^{\mathrm{D}n-2}$	$\mathrm{p}K_{\mathrm{TS}n}$
0	$(8.6 \pm 1.1) \times 10^{-22}$	3.1×10^{-1}			
1	$(5.2 \pm 0.2) \times 10^{-10}$	4.2×10^{3}	4.8×10^{-1}		11.78
2	$(1.0 \pm 1.8) \times 10^{-7}$	$<1.1 \times 10^{5}$	$<5.7 \times 10^{-6}$	$<1.3 \times 10^{7}$	<2.74
3	$(5.0 \pm 0.5) \times 10^{-4}$	$2.0 \times 10^{8}\ K_{\mathrm{D3}}$	5.0×10^{-4}	5.1×10^{2}	>3.25

$$k_{1\mathrm{obs}} = k_{\mathrm{P}}^{\mathrm{D1}}K_{\mathrm{D2}}K_{\mathrm{P1}} + k_{\mathrm{P1}}^{\mathrm{D}}K_{\mathrm{D1}}K_{\mathrm{D2}} \quad (31)$$

$$k_{2\mathrm{obs}} = k_{\mathrm{P}}^{\mathrm{D2}}K_{\mathrm{P1}} + k_{\mathrm{P1}}^{\mathrm{D1}}K_{\mathrm{D2}} + k_{\mathrm{P2}}^{\mathrm{D}}K_{\mathrm{D1}}K_{\mathrm{D2}}/K_{\mathrm{P2}} \quad (32)$$

$$k_{3\mathrm{obs}} = k_{\mathrm{P}}^{\mathrm{D3}}K_{\mathrm{P1}}/K_{\mathrm{D3}} + k_{\mathrm{P1}}^{\mathrm{D2}} + k_{\mathrm{P2}}^{\mathrm{D1}}K_{\mathrm{D2}}/K_{\mathrm{P2}} \quad (33)$$

The values of K_{D1}, K_{D2} and K_{P1} are substituted into eqn. (29) and the best fit values of the kinetic parameters, $k_{0\mathrm{obs}}$ to $k_{3\mathrm{obs}}$, and their standard deviations shown in Table 1 are obtained using non-linear least squares with proportional weighting to fit k_{obs} in eqn. (29). The curve corresponding to these best-fit values is shown in Fig. 6. The best-fit value of $k_{2\mathrm{obs}}$ is positive but less than its standard deviation and therefore it could be zero. This is reflected in the lack of a level region around pH 3 in Fig. 6. We have used the best-fit value plus one standard deviation as a best-fit upper limit of $k_{2\mathrm{obs}}$ used in subsequent calculations. Eqn. (30) allows the value of the rate constant $k_{\mathrm{P}}^{\mathrm{D}}$ shown in Table 1 to be calculated unambiguously. The second-order rate constants in each of eqns. (31) to (33) cannot be obtained unambiguously. For each eqn., however, all but one of each of the second-order rate constants is set to zero in turn and this enables an upper limit to be calculated for that one particular constant. These values are also shown in Table 1. The value of $k_{2\mathrm{obs}}$ is a best-fit upper limit, as described above, and values derived from this are indicated as such in Table 1. The value of $k_{\mathrm{P}}^{\mathrm{D3}}$ is dependent upon the unknown value of $K_{\mathrm{D3}} \geq 10$.

Transition state pK_a values

In multiple pathway reaction systems such as those leading to eqns. (31) to (33), where the second order rate constants cannot be obtained unambiguously, it is useful to apply the transition state pseudo-equilibrium constant approach developed by Kurz.[11] This yields transition state pseudo-equilibrium constant kinetic parameters, K_{TS}, that are independent of the actual pathway from reactants to products, *i.e.* independent of any proposed mechanism. The thermodynamic cycle shown in Scheme 3 represents the situation for the reaction of HOO^- and

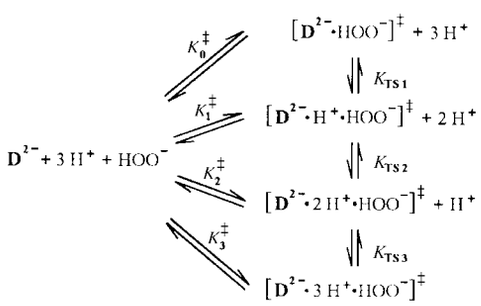

Scheme 3

D^{2-} in the presence of protons. Application of the transition state theory to the cycle leads to eqns. (34) to (36), where K_{TS1}, K_{TS2} and K_{TS3} are measures of the stabilisation imparted to the transition state as a result of association with one, two and three protons respectively. The pK_{TS} values calculated using eqns. (34) to (36) are shown in Table 1. Because $k_{2\mathrm{obs}}$ is a best-fit upper limit pK_{TS2} and pK_{TS3} are upper and lower limits, respectively.

$$K_{\mathrm{TS1}} = \frac{K_0^{\ddagger}}{K_1^{\ddagger}} = \frac{k_{0\mathrm{obs}}}{k_{1\mathrm{obs}}} \quad (34)$$

$$K_{\mathrm{TS2}} = \frac{K_1^{\ddagger}}{K_2^{\ddagger}} = \frac{k_{1\mathrm{obs}}}{k_{2\mathrm{obs}}} \quad (35)$$

$$K_{\mathrm{TS3}} = \frac{K_2^{\ddagger}}{K_3^{\ddagger}} = \frac{k_{2\mathrm{obs}}}{k_{3\mathrm{obs}}} \quad (36)$$

Discussion

It is important for the interpretation of the kinetics of dye oxidation that the solution structures of Green S are properly assigned in Scheme 1. The alkali bleached species is colourless and only the carbinol configuration, $\mathbf{D}(OH)^{3-}$, is possible. The relatively small spectral change (Figs. 1b and 2) in going from $\mathbf{D}^{2-}$ to $H\mathbf{D}^-$ around pH 7.66 (the pK_a of $H\mathbf{D}^-$) is consistent with retention of the $[Me_2NC_6H_4CC_6H_4NMe_2]^+$ chromophore[16] and protonation of the naphthyloxide oxygen.[17] The absorbance decrease (Figs. 1c, and 2) in going from $H\mathbf{D}^-$ to $H_2\mathbf{D}$ around pH 1.31 (the pK_a of $H_2\mathbf{D}$) indicates breaking of the chromophoric system due to protonation of an amine nitrogen.[18] The kinetic analysis must include $H_3\mathbf{D}^+$, eqn. (20), even though it is not spectrophotometrically detectable. There is no evidence from the kinetic or spectrophotometric data for the dye aggregation processes or buffer interactions seen with some other triarylmethane dyes.[19–21]

As well as HOO^- and H_2O_2, pK_a 11.6,[15] the kinetic analysis includes $H_3O_2^+$. The pK_a of the latter has been estimated[14] at −4.7 and so it is present at very low, but, potentially, kinetically significant concentrations under the present experimental conditions.[22] We have found no evidence of trace metal catalysed reactions involving the peroxide and the dye.

It is well accepted that the initial product of the peroxide bleaching of triarylmethane dyes by HOO^- is the dye hydroperoxide formed by attack on the central carbon.[4,9,10,23–26] The changes in the absorbance spectrum of Green S during peroxide bleaching at pH 12.4 are very similar to those between pH 2.4 and 9.7 (see Fig. 5). This is consistent with attack of peroxide on the central carbon in the latter pH range also. Besides this, the rate constant maximum, shown in Fig. 6, is much too high to be attributed to the alternative reaction, N-oxidation, involving nucleophilic attack of an amine nitrogen of the dye on H_2O_2.[27] In contrast, at pH 1.2 the changes in the absorption spectrum of Green S during peroxide bleaching are very different to those at higher pH and are consistent with N-oxidation that breaks the $[Me_2NC_6H_4CC_6H_4NMe_2]^+$ chromophore in a similar way to the N-protonation observed for $H_2\mathbf{D}$. Detailed product studies of the alkaline oxidation of phenolphthalein, PP^{2-}, by hydrogen peroxide have been reported.[10] These suggest that, after the initial rate-determining formation of the triphenylmethane dye hydroperoxide, inferred from the kinetic data, a rearrangement occurs, followed by further peroxidation and fragmentation of the dye. Since the present study is concerned only with the rate-determining attack of hydrogen peroxide on Green S, product studies are unnecessary at this stage.

Table 2 Equilibrium and rate constants for alkali bleaching and rate constant for hydroperoxide anion bleaching of Green S[a] and related[b] dyes

Dye	pK_{H_2O}	k_{HO^-}/dm^3 mol^{-1} s^{-1}	k_{H_2O}/s^{-1}	k_{HOO^-}/dm^3 mol^{-1} s^{-1}
$\mathbf{D}^{2-}$	11.72	$<4 \times 10^{-4}$	1.27×10^{-4}	3.1×10^{-1}
$\mathbf{BPB}^{2-}$	10.4	8.7×10^{-4}	$<1 \times 10^{-5}$[c]	2.4
PRDME	1.2	76	2.80×10^{-2}	3.0×10^{4}
$\mathbf{DAMS}^{+}$	0.2	450	8.7×10^{-2}	1.3×10^{5}

[a] Present work. [b] From ref. 23. [c] This generous upper limit for k_{H_2O} for Bromophenol Blue is taken as half the lowest point in the range of observed first-order rate constants quoted in ref. 23 corresponding to the lowest point in the range of hydroxide concentrations.

Exceptional reactivity of Green S (D^{2-}) and H_2O

The rate constant for the attainment of equilibrium during the alkali bleaching of Green S, $\mathbf{D}^{2-}$, increases with increasing hydrogen ion concentration as shown in Fig. 4. This unusual feature is explained using the conventional data treatment, eqns. (9) to (13), in terms of a high ratio of k_{H_2O} to k_{HO^-}. Table 2 compares values of pK_{H_2O}, k_{OH^-}, and k_{H_2O}, for the equilibration of $\mathbf{D}^{2-}$ and $\mathbf{D}(OH)^{3-}$, and k_P^D, k_{HOO^-}, for the reaction of the hydroperoxide anion and $\mathbf{D}^{2-}$, with the corresponding parameters for the structurally related series of dyes 4′,4″-dimethoxy-2-(methylsulfonyl)tritylium cation, $\mathbf{DAMS}^{+}$, Phenol

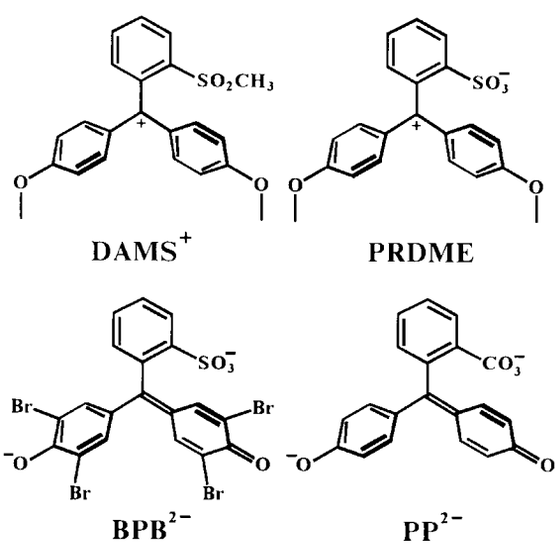

Red dimethyl ether zwitterion, **PRDME**, and Bromophenol Blue dianion, $\mathbf{BPB}^{2-}$.[23] Fig. 7 shows the corresponding plots of the logarithm of the rate constants against pK_{H_2O}. Linear relationships between log k_{HOO^-} and log k_{HO^-}, respectively, and pK_{H_2O} are observed. The reaction with HOO^- is considerably faster than with HO^-, in keeping with the α-nucleophilicity of HOO^- as seen with other polyarylmethane dyes including Malachite Green, Pyronin and 4-dimethylaminophenyltropylium.[24–26] In contrast to the linear relationships with HOO^- and HO^-, the rate constant for the reaction of water and Green S is about three orders of magnitude greater than expected from the values for the other dyes. The exceptionally high rate constant for the water reaction will be discussed after consideration of the exceptional reactivity of Green S and H_2O_2.

Transition state pseudo-equilibrium constants

The transition state pseudo-equilibrium constant approach of Kurz has found recent applications, discussed by More O'Ferrall and co-workers.[11,28,29] In the present work the triangular thermodynamic cycles of Scheme 3 differ in form but not principle[11] from the more usual rectangular cycle that would include the acid dissociation equilibria of the reactant species, eqns. (2)–(4), (24) and (25), explicitly. Using the triangular form to obtain the acid dissociation constant of the transition state allows a direct comparison with the independently measured

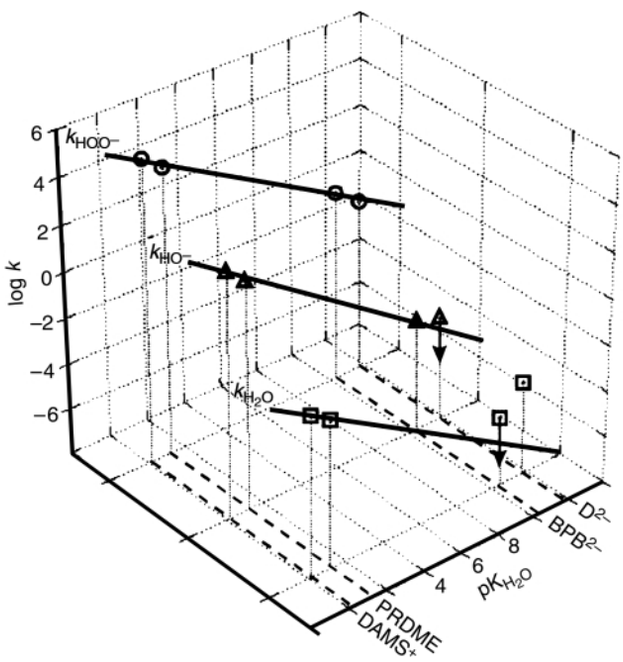

Fig. 7 Relationship between rate constants and pK_{H_2O} for a series of dyes, 4′,4″-dimethoxy-2-(methylsulfonyl)tritylium ion ($\mathbf{DAMS}^{+}$), Phenol Red dimethyl ether (**PRDME**), Bromophenol Blue ($\mathbf{BPB}^{2-}$) and Green S ($\mathbf{D}^{2-}$): circles, log (k_{HOO^-}/dm^3 mol^{-1} s^{-1}); triangles, log (k_{HO^-}/dm^3 mol^{-1} s^{-1}); squares, log (k_{H_2O}/s^{-1}).

acid dissociation constants of the reactants. This constitutes a comparison of the stabilisation of the transition state and reactants by a proton. We have previously used the triangular thermodynamic cycles to compare the stabilisation of reactants and transition states by cyclodextrin.[30] In the present work, pK_{TS} values are used to distinguish between attack of HOO^- on $H\mathbf{D}^-$ and attack of H_2O_2 on $\mathbf{D}^{2-}$ (see following section). Also, a characteristic pK_{TS} for the reaction of $H_3O_2^+$ and $H\mathbf{D}^{-1}$ is obtained (see final section).

Exceptional reactivity of Green S (D^{2-}) and H_2O_2

Table 1 shows that the value of k_{1obs} is commensurate with a rate constant of 0.48 dm^3 mol^{-1} s^{-1} for the reaction of hydrogen peroxide with $\mathbf{D}^{2-}$ or 4.2×10^3 for the reaction of HOO^- and $H\mathbf{D}^-$. The exceptional reactivity of $\mathbf{D}^{2-}$ and H_2O, described above, provides a compelling argument for the existence of a reaction between $\mathbf{D}^{2-}$ and H_2O_2 since H_2O_2 is a much better nucleophile than H_2O. The consideration of pK_{TS} values that follows provides further evidence that the reaction between $\mathbf{D}^{2-}$ and H_2O_2 predominates. The apparent pK_a of the singly protonated transition state pK_{TS1}, 11.78, given in Table 1, compares with the pK_{P1} of H_2O_2, 11.6, and the pK_{D1} of $H\mathbf{D}^-$ of 7.66. If the transition state involved attack of HOO^- on $H\mathbf{D}^-$ protonated on the oxygen then the approach of the negatively charged nucleophile would be expected to raise the pK_a of the OH in the transition state by no more than about 1.2 pH units compared to its value in the dye, on electrostatic grounds.[11b] This is clearly not the case. On the other hand, from electro-

static considerations, the negative charge on the O^- of $\mathbf{D}^{2-}$ would raise the pK_a of HOOH in the transition state involving these species by no more than 1.2 pH units. Moreover, for early transition states involving little bond formation between the good nucleophiles HOOH or HOO^- and the central carbon, there would not be much development of positive charge on the attacking oxygen and only a small decrease in the pK_a of a transition state involving HOOH and $\mathbf{D}^{2-}$. The observed result is consistent with the two small opposing factors more or less cancelling and we can conclude the predominant pathway involves H_2O_2 and $\mathbf{D}^{2-}$ with a rate constant (not statistically corrected for the two equivalent nucleophilic O atoms) k_{P1}^{D} 0.48 $dm^3\ mol^{-1}\ s^{-1}$. This is similar to the rate constant for the reaction between HOO^- and $\mathbf{D}^{2-}$, k_P^D 0.31 $dm^3\ mol^{-1}\ s^{-1}$. It is unusual for H_2O_2 to have a similar nucleophilic reactivity to HOO^-. However, the exceptional reactivity of H_2O_2 and $\mathbf{D}^{2-}$ mirrors that of H_2O and $\mathbf{D}^{2-}$ and will be discussed in the next section.

In order to quantify the exceptional reactivity of hydrogen peroxide and $\mathbf{D}^{2-}$ it is necessary to obtain an estimate for the rate constant for reaction of H_2O_2 and $H\mathbf{D}^-$. Table 1 shows the various second-order rate constants corresponding to k_{2obs} for transition states involving HOO^-, $\mathbf{D}^{2-}$, and two additional protons. As described in the results section it is not possible to obtain k_{2obs} with any confidence because it is so small compared to k_{1obs} and k_{3obs}, nevertheless a best-fit upper limit of k_{2obs} was obtained. This enables a lower limit for the ratio k_{P1}^{D}/k_{P1}^{D1} of $>7.9 \times 10^4$ to be estimated. This holds true irrespective of the actual pathway of the reaction involving two protons, since if the k_{2obs} reaction does not involve predominantly H_2O_2 and $H\mathbf{D}^-$ then k_{P1}^{D}/k_{P1}^{D1} would be even higher. Similarly, the corresponding upper limit of the pK_a of the transition state involving two additional protons, pK_{TS2}, <2.74 can be calculated and applied to the reaction between H_2O_2 and $H\mathbf{D}^-$ irrespective of the predominant pathway. The above value is considerably less than the pK_a of the transition state involving one additional proton and is consistent with attack of H_2O_2 on the central carbon of $H\mathbf{D}^-$ where in the absence of intramolecular base catalysis there is a later transition state and much more development of positive charge on the attacking peroxide oxygen, resulting in weaker binding of the attached proton.

Intramolecular catalysis

It has been shown that the rate constant for the attack of H_2O on Green S, $\mathbf{D}^{2-}$, is about three orders of magnitude greater than that expected from the values of the rate constant for a series of structurally related dyes. Yet the rate constants for the reactions of HO^- and HOO^- with Green S and the other dyes are in line. The rate constants for the reactions of HOO^- and H_2O_2 with $\mathbf{D}^{2-}$ are very similar whilst, for example, the rate constant for the reaction of HOO^- and phenolphthalein (0.156 $dm^3\ mol^{-1}\ s^{-1}$) is almost two orders of magnitude greater than that of H_2O_2.[10] The rate constant for the reaction of H_2O_2 and $\mathbf{D}^{2-}$ is at least about five orders of magnitude greater than that of H_2O_2 and $H\mathbf{D}^-$, protonated at the naphthyloxide oxygen, Scheme 1. All of these comparisons point to intramolecular base catalysis by the naphthyloxide O^- *ortho* to the central carbon site of attack of H_2O_2 and H_2O, especially since the attack of H_2O on polyarylmethane substrates is subject to general base catalysis.[3,4,31,32] Fig. 8 shows that the *ortho*-O^- is suitably orientated to remove a proton from the attacking H_2O_2, forming a six-membered ring in the activated complex. A similar activated complex can be envisaged for the water reaction. (Molecular models likewise show that there is sufficient space on the side of the central carbon opposite to the *ortho*-O^- to allow attack of HOO^- from this more electrostatically favoured position.) Not only is the *ortho*-O^- correctly located to remove a proton from the attacking H_2O_2 but also its conjugate acid has a pK_a 7.66 (pK_{D1} for $H\mathbf{D}^-$) well below that of hydrogen peroxide yet well above that expected for the initial product of reaction of H_2O_2 and other polyarylmethane dyes, $[H_2O_2^+–CR_3]$. These are the conditions necessary for concerted general base catalysis proposed by Jencks.[33] It is also relevant that the pK_a of $H\mathbf{D}^-$ is close to that of the imidazolinium ion, 7.0, whose conjugate base in the distal histidine of peroxidases functions in part to remove a proton from the incoming hydrogen peroxide during the formation of the active intermediate at neutral pH.[6] A further function of the imidazolinium ion is to donate its proton to the hydroxylic peroxide oxygen in order to facilitate heterolytic cleavage of the oxygen–oxygen bond with the release of H_2O, a good leaving group.[6] It is interesting to speculate whether during dye oxidation under conditions of pH where the *ortho*-O^- is protonated it acts as a general acid catalyst in a similar manner to the imidazolinium of peroxidase. It is well-known that protonation of the hydroxylic oxygen of hydroperoxides leads to oxygen–oxygen bond heterolysis followed by rearrangement.[34] Upon formation of the dye hydroperoxide the central carbon changes from sp^2 to sp^3 hybridisation and the *ortho*-OH takes a position closer to the hydroxylic oxygen of the peroxide, thus facilitating oxygen–oxygen bond cleavage by the formation of $[H_2O^+–OCR_3]$ in an intramolecular acid catalysed step.

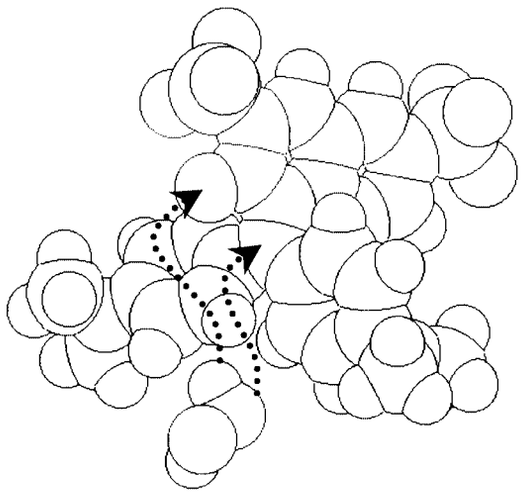

Fig. 8 Space-filling representation of the attack of H_2O_2 on $\mathbf{D}^{2-}$, orientation of dye as in graphical abstract.

Reaction of Green S ($H\mathbf{D}^-$) and $H_3O_2^+$

At pH 1.2 the changes in the absorption spectrum of Green S during peroxide bleaching are very different to those at higher pH and are consistent with N-oxidation that disrupts the main absorbance band in a similar way to that observed for $H_2\mathbf{D}$, rather than attack at the central carbon. This rules out reactions involving $H_3\mathbf{D}^+$ or $H_2\mathbf{D}$ since these have no lone pair of electrons on the nitrogen necessary for N-oxidation. Hence the k_{3obs} term must represent predominantly the reaction of $H\mathbf{D}^-$ and $H_3O_2^+$ giving the corresponding rate constant, k_{P2}^{D1}, shown in Table 1. A lower limit of pK_{TS3} > 3.21 is calculated using the best-fit upper limit of k_{2obs} and the best-fit value of k_{3obs}. Following a similar argument to the one used previously, the lower limit of pK_{TS3} holds irrespective of the predominant pathway for the ill-defined k_{2obs} reaction. The recent compilation by Edwards[22] of second and third order rate constants for the reactions of H_2O_2 and $H_3O_2^+$, respectively, with nucleophiles yields values of pK_{TS} in the region 1 to 4, the higher values being observed for nucleophiles with lower second order rate constants. The calculated lower limit of pK_{TS3} is in line with this.

Changes in the absorption spectrum of Green S during bleaching by peracids over a wide range of pH are similar to those observed with $H_3O_2^+$ at pH 1.2.[35] This is consistent with

N-oxidation and the good leaving group properties of H_2O and the parent acid anion of the peracid.

Acknowledgement

We thank Dr Alan M. Jones for helpful discussions.

References

1 Y. Yang, D. T. Wyatt and M. Bahorsky, *Text. Chem. Color.*, 1998, **30**, 27.
2 J. E. Gwinn and D. C. Bomberger, *Wastes From Manufacture of Dyes and Pigments. Vol. 5. Diphenylmethane and Triarylmethane Dyes and Pigments*; US EPA-600/2-84-111e; US Government Printing Office: Washington, DC, June 1984.
3 Y. Tsuno and M. Fujio, *Adv. Phys. Org. Chem.*, 1999, **32**, 267.
4 C. D. Ritchie, *Can. J. Chem.*, 1986, **64**, 2239.
5 J. Fernandez, J. Bandara, A. Lopez, P. Albers and J. Kiwi, *J. Chem. Soc., Chem. Commun.*, 1998, 1493.
6 M. Wirstam, M. R. A. Blomberg and P. E. M. Siegbahn, *J. Am. Chem. Soc.*, 1999, **121**, 10178; T. L. Poulos and J. Kraut, *J. Biol. Chem.*, 1980, **255**, 8199.
7 H. C. Kelly, D. M. Davies, M. J. King and P. Jones, *Biochemistry*, 1977, **16**, 3543.
8 J. Oakes and P. Gratton, *J. Chem. Soc., Perkin Trans. 2*, 1998, 1857; J. Oakes P. Gratton, R. Clark and I. Wilkes, *J. Chem. Soc., Perkin Trans. 2*, 1998, 2569.
9 K. M. Thompson, W. P. Griffith and M. Spiro, *J. Chem. Soc., Chem. Commun.*, 1992, 1600; *J. Chem. Soc., Faraday Trans.*, 1993, **89**, 4035.
10 K. M. Thompson, W. P. Griffith and M. Spiro, *J. Chem. Soc., Faraday Trans.*, 1993, **89**, 1203.
11 (*a*) J. L. Kurz, *J. Am. Chem. Soc.*, 1963, **85**, 987; (*b*) *Acc. Chem. Res.*, 1972, **5**, 1.
12 J. Chodosh, R. D. Dix, R. C. Howell, W. G. Stroop and S. C. G. Tseng, *Invest. Ophthalmol. Visual Sci.*, 1994, **35**, 1046.
13 R. Hofmann, R. C. Andrews and Q. Ye, *Environ. Technol.*, 1998, **19**, 761; B. Chiswell and K. R. O'Halloran, *Analyst*, 1991, **116**, 657.
14 R. Curci, A. Giovine and G. Modena, *Tetrahedron*, 1966, **22**, 1235.
15 A. J. Everett and G. J. Minkoff, *Trans. Faraday Soc.*, 1953, **49**, 410.
16 P. F. Gordon and P. Gregory, *Organic Chemistry in Colour*, Springer-Verlag, Berlin, 1983; S. F. Beach, J. D. Hepworth, P. Jones, D. Mason, J. Sawyer, G. Hallas and M. M. Mitchell, *J. Chem. Soc., Perkin Trans. 2*, 1989, 1087.
17 D. F. Duxbury, *Chem. Rev.*, 1993, **93**, 381; S. G. R. Guinot, J. D. Hepworth and M. Wainwright, *J. Chem. Soc., Perkin Trans. 2*, 1998, 297; M. J. S. Dewar, *J. Chem. Soc.*, 1950, 2329; J. Griffiths, *Colour and Constitution of Organic Molecules*, Academic Press, London, 1976.
18 S. F. Beach, J. D. Hepworth and D. Mason, *J. Chem. Soc., Perkin Trans. 2*, 1983, 975.
19 H. B. Lueck, B. L. Rice and J. L. McHale, *Spectrochim. Acta*, 1992, **48A**, 819; W. H. J. Stork, G. J. M. Lippitis and M. Mandel, *J. Phys. Chem.*, 1972, **76**, 1772; M. Takatsuki, *Bull. Chem. Soc. Jpn.*, 1980, **53**, 1922; N. A. Gracheva, D. S. Lychnikov and E. N. Dorokhova, *J. Anal. Chem. USSR*, 1989, **44**, 691.
20 J. C. Turgeon and V. K. La Mer, *J. Am. Chem. Soc.*, 1952, **74**, 5988.
21 S. A. Lomonosov, N. I. Shukolyukova and L. D. Krupkina, *J. Anal. Chem. USSR*, 1974, **29**, 1095; S. A. Lomonosov, *J. Anal. Chem. USSR*, 1973, **28**, 1469.
22 R. Curci and J. O. Edwards, in *Catalytic Oxidations with Hydrogen Peroxide as Oxidant*, ed. G. Strukul, Kluwer Academic Publishers, Dordrecht, 1992, p. 45.
23 C. D. Ritchie and T. C. Hofelich, *J. Am. Chem. Soc.*, 1980, **102**, 7039.
24 J. E. Dixon and T. E. Bruice, *J. Am. Chem. Soc.*, 1971, **93**, 6592.
25 C. D. Ritchie, C. Kubisty and G. Y. Ting, *J. Am. Chem. Soc.*, 1983, **105**, 279.
26 C. D. Ritchie, R. J. Minasz, A. A. Kamego and S. Sawada, *J. Am. Chem. Soc.*, 1977, **99**, 3747.
27 K. M. Ibne-Rasa and J. O. Edwards, *J. Am. Chem. Soc.*, 1962, **84**, 763; S. D. Ross, *J. Am. Chem. Soc.*, 1946, **68**, 1484.
28 G. Ercolani and L. Mandolini, *J. Am. Chem. Soc.*, 1990, **112**, 423.
29 S. J. Eustace, G. M. McCann, R. A. More O'Ferrall, M. G. Murphy, B. A. Murray and S. M. Walsh, *J. Phys. Org. Chem.*, 1998, **11**, 519.
30 D. M. Davies and M. E. Deary, *J. Chem. Soc., Perkin Trans. 2*, 1996, 2423; 1999, 1027.
31 R. A. McClelland, U. M. Kanagasabapathy, N. S. Banait and S. Steenken, *J. Am. Chem. Soc.*, 1989, **111**, 3966.
32 C. D. Ritchie, *J. Am. Chem. Soc.*, 1972, **94**, 3275; C. D. Ritchie, D. J. Wright, D.-S. Huang and A. A. Kamego, *J. Am. Chem. Soc.*, 1975, **97**, 1163.
33 W. P. Jencks, *J. Am. Chem. Soc.*, 1972, **94**, 4731.
34 R. Hiatt, in *Organic Peroxides*, ed. D. Swern, Wiley, New York, 1971, p. 1.
35 D. M. Davies and A. U. Moozyckine, unpublished results.